Article

Synthesis and Characterization of Photo-Responsive Thermotropic Liquid Crystals Based on Azobenzene

Runmiao Yang *, Dejian Zhao, Guanxiu Dong, Yuhai Liu and Danting Wang

School of Material Engineering, Jiangsu University of Technology, Changzhou 213001, China; zdj@jsut.edu.cn (D.Z.); dxdgx@jsut.edu.cn (G.D.); lyh@jsut.edu.cn (Y.L.); summerwdt@163.com (D.W.)
* Correspondence: yangrunmiao@jsut.edu.cn; Tel.: +86-0519-8695-3292

Abstract: A series of new thermotropic liquid crystals (LCs) containing azobenzene units was synthesized. The structures of the compounds were characterized by means of NMR and FTIR spectroscopy. Their mesomorphic behaviors were investigated via differential scanning calorimetry (DSC) and polarizing optical microscopy (POM). Based on the POM and DSC measurements, the optical properties of the Razo-ester were tested using UV-vis spectroscopy. The azobenzene side chain displayed a strong ability to influence the formation of thermotropic LCs.

Keywords: azobenzene; liquid crystals; photo-responsive behaviors

1. Introduction

Liquid–crystalline materials have been applied for optical information displays and storage devices, as the modulation of the liquid-crystalline phase's molecular alignment can be controlled by external stimuli, such as heat, electric fields, and light [1–3]. Azobenzene and its derivatives are photoisomerizable materials that undergo a reversible transformation between *trans* and *cis* isomers in the presence of light. Liquid crystals (LCs) containing an azobenzene moiety, either of low molar mass or polymeric in nature, have attracted tremendous attention as a result of their light-induced, photo-switchable, and elastic properties [4–6]. The introduction of reversible *trans–cis* photoisomerization of azobenzene can exert large effects on the properties of LCs [7–10].

In recent times, study of LC's incorporation of azobenzene moiety has been developing [11,12]. For example, Tomczyk synthesized a new class of star-shaped, liquid-crystalline functionalized with photochromic azobenzene and mesogenic groups, and investigated its light-induced anisotropy [13]. Zupančič studied the phenomenon of laser beam propagation in azobenzene liquid crystals (azo LCs) in waveguiding configuration [14]. Yamamoto investigated the viscoelastic and photoresponsive properties of composite gels through the *cis–trans* photoisomerization of the azobenzene compound doped into the host LCs [15].

Although a variety of azobenzene compounds are now used in the formulation of the thermochromic LC, the influence of the side chain of the azobenzene moiety, which ensures the stable formation of LCs remains rare [16,17]. Ahmed reported the mesophase behavior of 1:1 mixtures of 4-n-alkoxy phenylazo benzoic acids bearing terminal alkoxy groups of different chain lengths.

As we know, the properties of an LC depend on the chemical structure of the azobenzene and other segments [18]. With those objects in mind, we designed and synthesized a new series of azobenzene LC compounds, containing a flexible chain of C_mH_{2m} (where m = 4–12). In addition, a sequence of very interesting phase changes were observed when the compounds were assigned to different terminal groups, such as alkyloxy, alkoxy, ester, and hydroxyl. The phase behaviors of these compounds were characterized by differential scanning calorimetry (DSC) and polarizing optical microscopy (POM). The compounds of these series exhibited different phases when changing

temperature. This investigation revealed that the kind of chain at the side of the azobenzene moiety plays a more important role in the formation of LC phases than has previously been understood.

2. Materials and Methods

2.1. Chemicals and Characterization

All chemicals were purchased from Sigma-Aldrich (New York, NY, USA) and Merck (Berlin, Germany), and used without further purification. All the chemicals were characterized by ^{1}H and ^{13}C NMR spectroscopy on a 400 MHz Bruker Ultrashield Spectrometer (Bruker, Germany) in CDCl$_3$. Accurate mass spectra were obtained on a Thermo Scientific Q Exactive FTMS, employing an ASAP probe (Thermo Fisher Scientific, Waltham, MA, USA). Photoisomerization was measured on a Cary 50-Bio UV-Vis Spectrophotometer (Varian, Santa Clara, CA, USA) against a background of solvent in a quartz cuvette. *Trans* to *cis* isomerization was induced by an EXFO Acticure 4000 light source via a liquid light-guide working at 365 nm wavelength. The UV light intensity was about 3.8 mW/cm^2. *Cis* to *trans* isomerization was induced by visible light at 12.1 mW/cm^2. UV-vis data was collected every 30 s. POM was conducted using a Nikon Eclipse 80i (Nikon, Tokyo, Japan). Phase transition temperatures and enthalpies of discogens were investigated using a TA-DSC Q100 instrument (TA Instruments, New Castle, DE, USA) under N$_2$ atmosphere with heating and cooling rates of 10 °C min^{-1}.

2.2. Synthesis of Target Compounds

Compound 1:8.9 g of ethyl p-aminobenzoate was dissolved in 80 mL of 12% solution of hydrochloric acid. Solution was cooled to 0 °C in an ice bath. Then 4.5 g of sodium nitrite in 30 mL of distilled water was added within 30 min. 6.2 g of phenol was added. After 1 h, 200 mL of a saturated solution of sodium carbonate was added. Resulting mixture was cooled. The precipitate was filtered off on a Büchner funnel. The product was isolated through recrystallization with ethanol. The powder obtained had a red-orange intense color, and was dried in a vacuum.

Yield: 65%. Mp: 162 °C. ^{1}H NMR (CDCl$_3$), δ (ppm): 1.39–1.42 (t, 3H, CH$_3$), 4.37–4.42 (q, 2H, CH$_2$), 6.94–6.96 (d, 2H, Ar-H), 7.87–7.91 (q, 4H, Ar-H), 8.15–8.17 (d, 2H, Ar-H).

Compound 2a: Compound 1 (9.2g), anhydrous K$_2$CO$_3$ (9.4 g) and KI (0.18 g) were dissolved in 120 mL of acetone, under argon atmosphere. After 10 min stirring, 1-bromobutane (5.6g) was added dropwise via syringe while the solution was refluxing. The mixture was stirred overnight under reflux. After cooling down to room temperature, 200 mL of water was added. The product was extracted with dichloromethane. The organic layer was dried with MgSO$_4$ and filtered, and then the solvent was evaporated. The product was recrystallized with ethanol. Yield: 86%. The product was an orange powder.

Yield: 86%. Mp: 87 °C. HRMS = 383.2323. ^{1}H NMR (CDCl3) δ (ppm): 0.86–0.89 (t, 3H, CH3), 1.28–1.52 (m, 13H, CH$_2$, CH$_3$), 1.78–1.84 (quint, 2H, CH$_2$), 4.02–4.05 (t, 2H, OCH$_2$), 4.36–4.42 (q, 2H, COOCH$_2$), 6.98–7.00 (d, 2H, Ar-H), 7.87–7.92 (q, 4H, Ar-H), 8.15–8.17 (d, 2H, Ar-H). ^{13}C NMR (CDCl$_3$), 166.32, 162.48, 155.49, 147.00, 131.63, 130.69, 125.34, 125.34, 122.46, 114.94, 77.51, 77.19, 76.87, 68.59, 61.33, 31.97, 29.51, 29.39, 29.33, 26.17, 22.82, 14.51, 14.27.
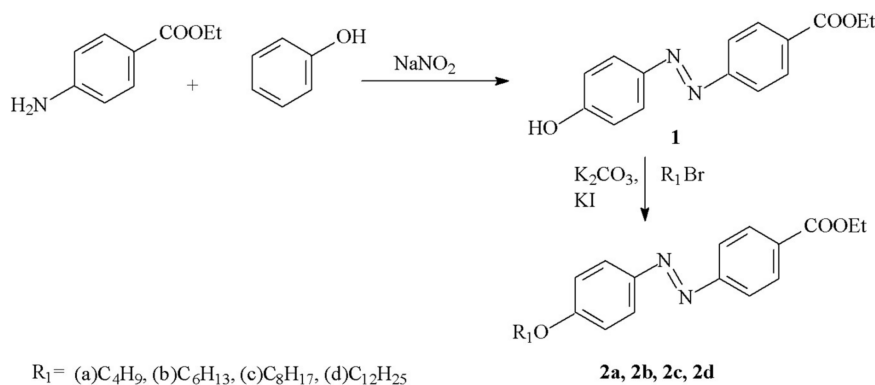
Compound 2b–d was synthesized according to the same method used for compound 2a. ^{1}H NMR data was shown in Figure 1. Compound 3a–c was synthesized in accordance with the literature and our previous works. Data are not shown here [17–21].

3. Results

3.1. Synthesis and Characterization

The synthetic route for compounds 2a–d with azobenzene moiety and different side chains is outlined in Scheme 1. The chemical structures of these compounds were characterized using

a combination of ^{1}H NMR and FTIR spectroscopy. Protons in the structure of compounds 2a–d were denoted by the letters "a–i" as shown in Figure 1. For the compound **2a** with C_4 alkyl chain, the chemical shift around δ = 6.90–8.30 ppm corresponds to the proton from the azobenzene moiety, while the peaks at δ = 3.90–4.10 and δ = 5.35–5.60 correspond to methine protons (Figure 1a). As the alkyl chain of compounds 2a–d increased from C_4 to C_6, an obvious increase of the chemical shift for the CH_2 proton around 1.3 ppm was observed. As the alkyl chain further increased to C_8 and C_{12} for the compounds 2c–d, the corresponding increase of the shift was observed, which proved the compounds had been synthesized successfully.

R_1 = (a)C_4H_9, (b)C_6H_{13}, (c)C_8H_{17}, (d)$C_{12}H_{25}$ **2a, 2b, 2c, 2d**

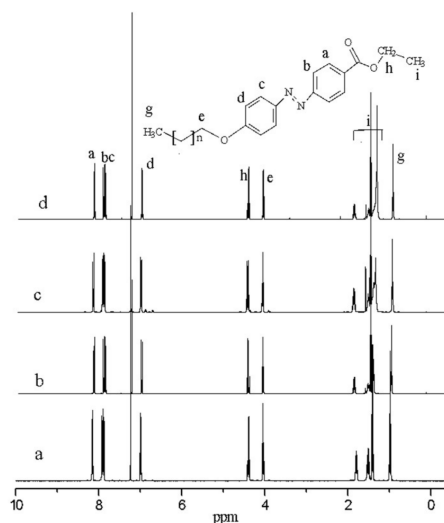**Scheme 1.** Synthetic scheme of compounds 2a–d.

Figure 1. ^{1}H NMR spectra of compound 2a–d.

The chemical structures of compounds 2a–d were confirmed by the FTIR results. As shown in Figure 2, the absorption occurs at 1730 cm^{-1}, which is attributed to the carbonyl group of the compounds. The absorption occurs at 1600 cm^{-1} corresponding to the benzene skeleton vibration in the spectrum of azobenzene. The FTIR bands at 2930 and 2850 cm^{-1} represent the anti-symmetrical and symmetrical stretch vibrations and absorption spectra of CH_2 group, respectively. An increase in the absorption intensity of the CH_2 group was observed, which illustrates the difference between the compounds. The presence of the above bands in the graft copolymer gives strong evidence of successful synthesis.
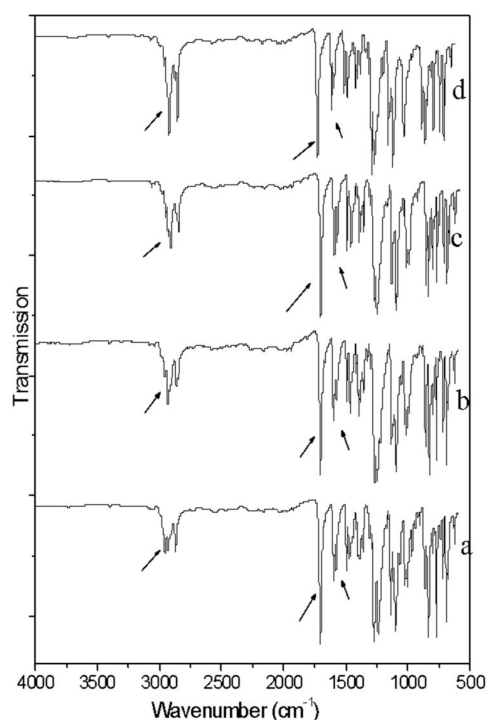
Figure 2. FTIR spectra of compound 2a–d.

3.2. Liquid Crystal Properties of the Synthesized Cm-Azo-Ester

The structures of obtained compounds used in this paper are shown in Scheme 1. A POM with a heating stage and DSC were used for measuring the melting temperature (*Tm*) and isotropization temperature (*Ti*) of the compounds. DSC thermograms for compounds 2a–d upon heating and cooling cycles were shown in Figure 3. Compounds 2a–d exhibited similar phase transition behaviors. For example, in the DSC measurements of compound 2c (Figure 3c), an exothermic peak appeared at 103 °C when the compound was cooled from the molten state, confirming a phase transition from the isotropic phase to the nematic phase. Another exothermic peak at 64 °C was assigned to the crystallization. Further endothermic peaks were observed at 80 °C, which were attributed to nematic–smectic phase transitions.
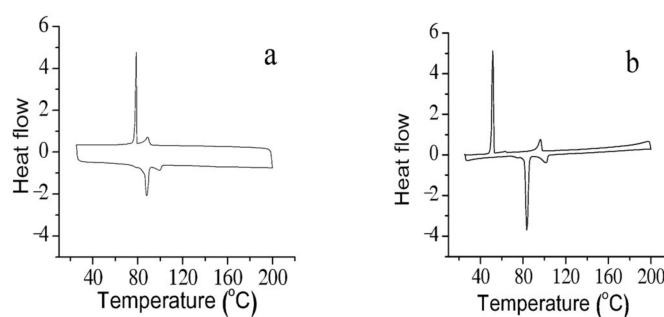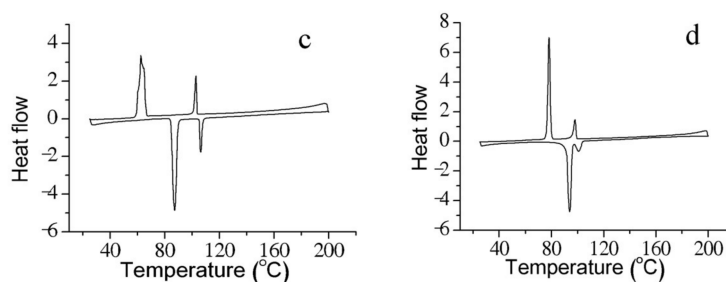

Figure 3. *Cont.*

Figure 3. DSC traces of (**a**) compound 2a; (**b**) compound 2b; (**c**) compound 2c; and (**d**) compound 2d.

Compound 2c was selected for the phase transition study by POM. Figure 4 shows representative POM micrographs of compound 2c at different temperatures. Birefringent texture for the crystalline phase was observed when the temperature was below 88 °C (Figure 4a). When the temperature was increased to 90 °C, POM texture of the enantiotropic smectic phase was formed (Figure 4b). Upon further heating, the phase transformed into another smectic phase with a typical fan-shaped texture. It should be noted that this transition was not observed by DSC measurement (Figure 4c). After increasing the temperature to 102 °C, the transition from a smectic to a nematic phase was observed (Figure 4d). The isotropic optical property was formed at 106 °C, indicated by the disappearance of brightness under polarized light (Figure 4e). When cooling down from melted isotropic liquid at a high temperature, birefringence emerged again due to the formation of a nematic phase (Figure 4f). Upon further cooling, the phase transformed into a smectic phase (Figure 4g), and finally, a solid crystal phase (spherulite texture) was regained at 64 °C (Figure 4h).
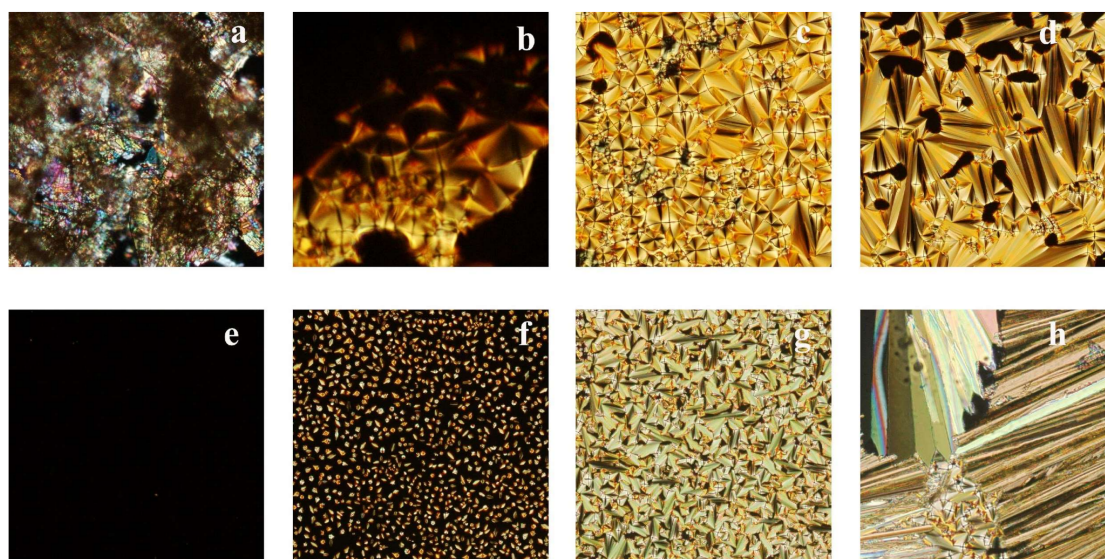

Figure 4. POM textures of compound 2c. (**a**) below 88 °C, crystal; (**b**) at 90 °C, smectic phase; (**c**) at 100 °C, smectic phase; (**d**) at 102 °C, transition smectic-nematic; (**e**) at 115 °C, isotropic phase; (**f**) cooled from isotropic liquid, at 102 °C, nematic phase; (**g**) at 80 °C, transition nematic-smectic; and (**h**) at 64 °C, transition smectic-crystal (100× magnification).
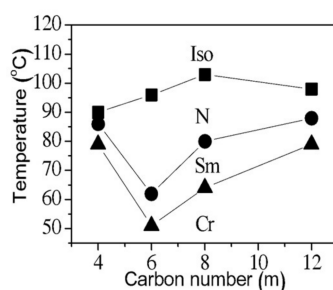
According to the results of the POM and DSC, the phase transition temperature results of the compounds 2a–d were listed in Table 1. The results show that all the compounds 2a–d have stable smectic–nematic phases with a broad temperature range, which is important for their potential application to the field of optoelectronics.

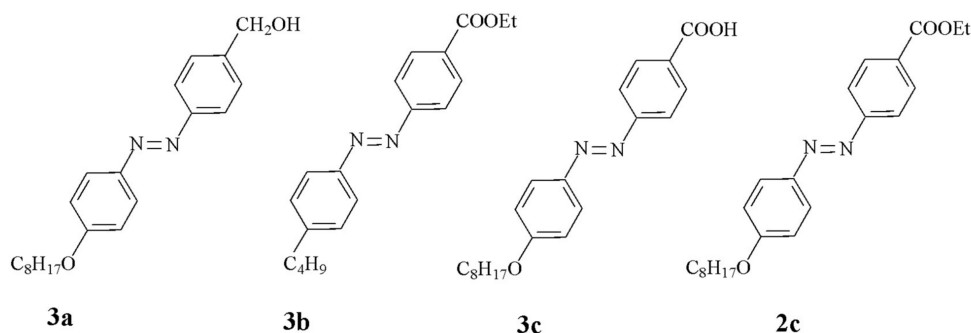**Table 1.** Phase transition temperatures (°C) of compounds 2a–d.

Compound	Phase Sequence	
	Heating	Cooling
2a	Cr 87 Sm 98 N 100 I	I 90 N 86 Sm 79 Cr
2b	Cr 84 Sm 96 N 101 I	I 96 N 62 Sm 51 Cr
2c	Cr 87 Sm 102 N 106 I	I 103 N 80 Sm 64 Cr
2d	Cr 94 Sm 96 N 101 I	I 98 N 88 Sm 79 Cr

Phase transition temperatures were determined by DSC thermogram. Cr, crystal; N, nematic; Sm, smectic; I, isotropic. Phase transition was observed by POM.

The correlation between the phase transition temperature and side chain length was summarized in Figure 5. One of the notable features was that when the side chain length changed from C_4H_9 to $C_{12}H_{25}$, the nematic phase temperature range was initially increased from C_6H_{13} to C_8H_{17}. After that, a descending trend was observed when the spacer changed from C_8H_{17} to $C_{12}H_{25}$. By contrast, in comparison to the temperature range of the nematic phase, the smectic phase temperature range had little influence on the side chain length from C_4H_9 to $C_{12}H_{25}$.

Figure 5. A plot showing the transition temperature as a function of spacer length on cooling.

In order to study the effect of molecular structure on the formation of LCs, we synthesized some compounds which have different functional groups on sides of azobenzene (Scheme 2). It has been reported that the molecular shape and the intermolecular force were important to the formation of liquid-crystalline phases [22]. Ester and ether on both sides of azobenzene can provide appropriate molecular interactions, such as hydrophobic interactions, π-π interactions, and van der Waals forces, which will promote the bonding between the donor and acceptor of the rigid parts, and hence increase the effective length of mesogenic groups. The increased effective length of rigid mesogenic groups can lead to the easy formation of liquid-crystalline phases. By contrast, when the type of groups on sides of azobenzene were changed, structure-property relationships in LC were observed. DSC and POM results showed that no liquid–crystalline phases were detected in compounds 3a–c. This is clearly demonstrated by the fact that the covalent incorporation groups on sides of azobenzene play an important role in stabilizing the LC phase.

Scheme 2. Molecular structure of compounds 3a–c and compound 2c.

3.3. UV-Visible Spectra

The early work has reported that LCs incorporating azobenzene moiety exhibit *trans–cis* photoisomerization behavior upon UV-Visible (UV-Vis) light irradiation [23,24]. Figure 6 shows the UV-induced *trans–cis* isomerization of compound 2c. Its reversible photoresponsive properties were well-demonstrated by in situ POM characterization. By irradiating the compound with UV light, it can be transformed from the anisotropic state to the isotropic state owing to the isomerization of azobenzene. Switching to visible light induced the expected return to the anisotropic phase. UV-Vis spectra were employed to evaluate the isomerization of compound 2c in solution during the reversible changes under alternating UV and visible light irradiation. For example, the UV-Vis spectra of compound 2c in CH_2Cl_2 solution are shown in Figure 7 (the concentration was 0.002 wt %). The data were obtained at a constant frequency of 30 s/time under UV light (365 nm, 3.8 mW/cm^2) or visible light (12.1 mW/cm^2). The compound exhibited an absorption maximum at 360 nm and weak shoulders at 440 nm, which were related to p–p* and n–p* transitions of the azobenzene *trans–cis* configuration, respectively [25].
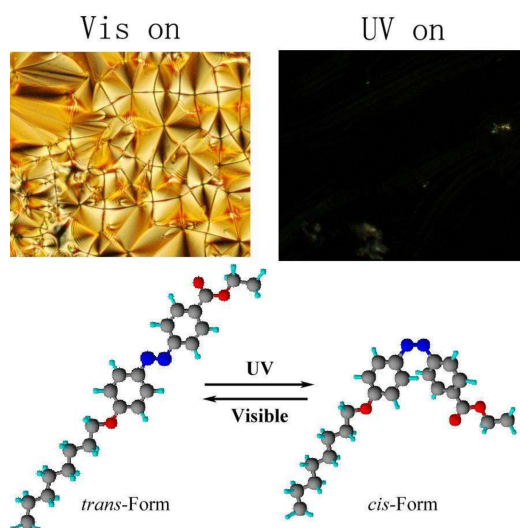

Figure 6. UV-induced *trans–cis* isomerization of compounds 2c (POM, 200× magnification), space filling model drawn by 3D-ChemDraw.
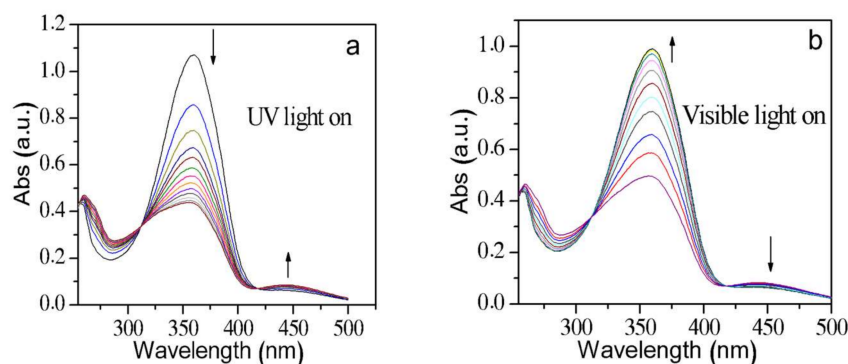

Figure 7. Compound 2c in CH_2Cl_2 at 20 °C (0.002 wt %), (**a**) change in absorption of UV-Vis spectra over time under UV light (365 nm, 3.8 mW/cm^2) and (**b**) change in absorption of UV-Vis spectra over time under visible light (12.1 mW/cm^2).

4. Discussion

A series of new LCs based on azobenzene was synthesized and their properties were studied through DSC and POM. The results show that the alkyloxy chains (m = 4–12) in the homologue lead to different phase changes at different temperatures. The compounds 2a–d have clear smectic–nematic phases within a broad temperature range, making them potentially applicable to the field of optoelectronics. Three other compounds which contain different substituent groups in the two sides of azobenzene have also been studied. DSC and POM studies revealed that these compounds do not exhibit any liquid crystallinity.

In addition to our findings, the results obtained here will act as feedback to assist us with ongoing research. We are continuing our synthesis work to find out if we can synthesize other examples of LCs based on azobenzene. Furthermore, we are developing methods in order to more efficiently predict materials with desirable applications.

Author Contributions: Dejian Zhao and Runmiao Yang conceived and designed the experiments; Yuhai Liu performed the experiments; Guanxiu Dong and Danting Wang analyzed the data; Runmiao Yang wrote the paper.

Conflicts of Interest: The authors declare no conflict of interest.

References

1. Rey, A.D.; Herrera-Valencia, E.E. Invited review liquid crystal models of biological materials and silk spinning. *Biopolymers* **2012**, *97*, 374–396. [CrossRef] [PubMed]
2. Miniewicz, A.; Orlikowska, H.; Sobolewska, A.; Bartkiewicz, S. Kinetics of thermal *cis–trans* isomerization in a phototropic azobenzene-based single-component liquid crystal in its nematic and isotropic phases. *Phys. Chem. Chem. Phys.* **2018**, *20*, 2904–2913. [CrossRef] [PubMed]
3. Akamatsu, N.; Hisano, K.; Tatsumi, R.; Aizawa, M.; Barrett, C.J.; Shishido, A. Thermo-, photo-, and mechano-responsive liquid crystal networks enable tunable photonic crystals. *Soft Matter* **2017**, *13*, 7486–7491. [CrossRef] [PubMed]
4. Gupta, M.; Gupta, S.P.; Mohapatra, S.S.; Dhara, S. Room-temperature oligomeric discotic nematic liquid crystals over a wide temperature range: Structure-property relationships. *Chemistry* **2017**, *23*, 10626–10631. [CrossRef] [PubMed]
5. Nardele, C.G.; Asha, S.K. Twin liquid crystals and segmented thermotropic polyesters containing azobenzene-effect of spacer length on lc properties. *J. Polym. Sci. Part A Polym. Chem.* **2012**, *50*, 2770–2785. [CrossRef]
6. Sato, M.; Nagano, S.; Seki, T. A photoresponsive liquid crystal based on (1-cyclohexenyl)phenyldiazene as a close analogue of azobenzene. *Chem. Commun.* **2009**, *25*, 3792–3794. [CrossRef] [PubMed]
7. Yeap, G.Y.; Balamurugan, S.; Rakesh, S. Synthesis and mesomorphic properties of chiral liquid crystal dimers derived from azobenzene and substituted naphthol. *Liq. Cryst.* **2013**, *40*, 555–563. [CrossRef]
8. Ryu, S.H.; Gim, M.J.; Lee, W.; Choi, S.W.; Yoon, D.K. Switchable photonic crystals using one-dimensional confined liquid crystals for photonic device application. *ACS Appl. Mater. Interfaces* **2017**, *9*, 3186–3191. [CrossRef] [PubMed]
9. Wang, G.J.; Zhang, M.Z.; Yang, Q.A.; Liu, F.; Cheng, Z.; Guo, R.; Yang, H. Photoinduced phase transitions in chiral binaphthyl-diol-doped smectic liquid crystals by a photochromic azobenzene. *Chem. Lett.* **2010**, *39*, 1144–1145. [CrossRef]
10. Fang, G.J.; Shi, Y.; Maclennan, J.E.; Clark, N.A.; Farrow, M.J.; Walba, D.M. Photo-reversible liquid crystal alignment using azobenzene-based self-assembled monolayers: Comparison of the bare monolayer and liquid crystal reorientation dynamics. *Langmuir* **2010**, *26*, 17482–17488. [CrossRef] [PubMed]
11. Wuckert, E.; Harjung, M.D.; Kapernaum, N.; Mueller, C.; Frey, W.; Baro, A.; Giesselmann, F.; Laschat, S. Photoresponsive ionic liquid crystals based on azobenzene guanidinium salts. *Phys. Chem. Chem. Phys.* **2015**, *17*, 8382–8392. [CrossRef] [PubMed]

12. Kim, D.Y.; Lee, S.A.; Park, M.; Choi, Y.J.; Kang, S.W.; Jeong, K.U. Multi-responsible chameleon molecule with chiral naphthyl and azobenzene moieties. *Soft Matter* **2015**, *11*, 2924–2933. [CrossRef] [PubMed]

13. Tomczyk, J.; Sobolewska, A.; Nagy, Z.T.; Guillon, D.; Donnio, B.; Stumpe, J. Photo- and thermal-processing of azobenzene-containing star-shaped liquid crystals. *J. Mater. Chem. C* **2013**, *1*, 924–932. [CrossRef]

14. Zupančič, B.; Diez-Berart, S.; Finotello, D.; Lavrentovich, O.D.; Zalar, B. Photoisomerization-Controlled Phase Segregation in a Submicron Confined Azonematic Liquid Crystal. *Phys. Rev. Lett.* **2012**, *108*, 257801. [CrossRef] [PubMed]

15. Yamamoto, T.; Yoshida, M. Viscoelastic and photoresponsive properties of microparticle/liquid-crystal composite gels: Tunable mechanical strength along with rapid-recovery nature and photochemical surface healing using an azobenzene dopant. *Langmuir* **2012**, *28*, 8463–8469. [CrossRef] [PubMed]

16. Peng, S.H.; Guo, Q.; Hughes, T.C.; Guo, Q. Controlling morphology and porosity of porous siloxane membranes through water content of precursor microemulsion. *Soft Matter* **2012**, *8*, 10493–10501. [CrossRef]

17. Ahmed, H.A.; Naoum, M.M.; Saad, G.R. Mesophase behaviour of 1:1 mixtures of 4-n alkoxyphenylazo benzoic acids bearing terminal alkoxy groups of different chain lengths. *Liq. Cryst.* **2016**, *43*, 1259–1267. [CrossRef]

18. Bisoyi, H.K.; Li, Q. Light-driven liquid crystalline materials: From photo-induced phase transitions and property modulations to applications. *Chem. Rev.* **2016**, *116*, 15089–15166. [CrossRef] [PubMed]

19. Yang, R.M.; Peng, S.H.; Wan, W.B.; Hughes, T.C. Azobenzene based multistimuli responsive supramolecular hydrogels. *J. Mater. Chem. C* **2014**, *2*, 9122–9133. [CrossRef]

20. Yang, R.M.; Peng, S.H.; Hughes, T.C. Multistimuli responsive organogels based on a reactive azobenzene gelator. *Soft Matter* **2014**, *10*, 2188–2196. [CrossRef] [PubMed]

21. Liu, D.; Broer, D.J. New insights into photoactivated volume generation boost surface morphing in liquid crystal coatings. *Nat. Commun.* **2015**, *6*, 8334. [CrossRef] [PubMed]

22. Kim, D.Y.; Lee, S.A.; Kim, H.; Kim, S.M.; Kim, N.; Jeong, K.U. An azobenzene-based photochromic liquid crystalline amphiphile for a remote-controllable light shutter. *Chem. Commun.* **2015**, *51*, 11080–11083. [CrossRef] [PubMed]

23. Shi, Y.; Fang, G.; Glaser, M.A.; Maclennan, J.E.; Korblova, E.; Walba, D.M.; Clark, N.A. Phase winding of a nematic liquid crystal by dynamic localized reorientation of an azo-based self-assembled monolayer. *Langmuir* **2014**, *30*, 9560–9566. [CrossRef] [PubMed]

24. Norikane, Y.; Uchida, E.; Tanaka, S.; Fujiwara, K.; Koyama, E.; Azumi, R.; Akiyama, H.; Kihara, H.; Yoshida, M. Photoinduced crystal-to-liquid phase transitions of azobenzene derivatives and their application in photolithography processes through a solid-liquid patterning. *Org. Lett.* **2014**, *16*, 5012–5015. [CrossRef] [PubMed]

25. Saint-Jalm, S.; Miniewicz, A.; Karpinski, P.; Jarek-Mikulska, U.; Galewski, Z. Photo-induced birefringence in a nematic liquid crystal mixture doped with light-switchable mesogenic azobenzene derivatives. *J. Mol. Liq.* **2012**, *168*, 21–27. [CrossRef]